18th International Conference on Information Fusion
Washington, DC - July 6-9, 2015

An extended target tracking model with multiple random matrices and unified kinematics

Karl Granström, Peter Willett, Yaakov Bar-Shalom
Department of Electrical and Computer Engineering, University of Connecticut, Storrs, Connecticut 06269
Email: karl@engr.uconn.edu, willett@engr.uconn.edu, ybs@engr.uconn.edu

***Abstract*—This paper presents a model for tracking of extended targets whose extent cannot be described by a simple geometric shape such as an ellipse or a rectangle. The extended target shape is represented by a number N_s of elliptic subobjects, where N_s is assumed known. Because an extended target is a rigid body, the subobject positions must necessarily be estimated as a single state with unified kinematics, and the full covariance matrix must be estimated. In addition to the position and kinematics, for each subobject the proposed model also estimates the number of measurements generated by the shape, as well as a random matrix as representation of the size and shape. A Gamma Gaussian inverse Wishart implementation is proposed, and the state prediction and update are given. A simulation study shows the merits of the model compared to extended target modeling without unified kinematics.**

***Index Terms*—Target tracking, extended target, group target, measurement rate, random matrix, gamma distribution, Gaussian distribution, inverse Wishart distribution.**

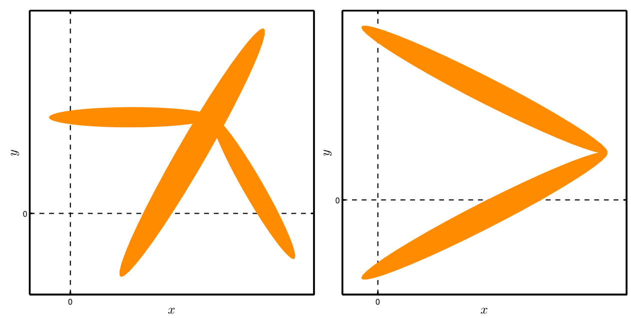

Fig. 1. Examples in 2D of extended/group targets that are represented by elliptic subobjects. Neither one of the examples has a shape that can be described by a simple geometric shape.

I. Introduction

Target tracking can be defined as the processing of a sequence of measurements obtained from a target in order to maintain an estimate of the target's current state. In this context an extended target is defined as a target that potentially gives rise to more than one measurement per time step. Closely related to an extended target is group target, defined as a cluster of point targets that cannot be tracked individually, but has to be treated as a single object. In extended target tracking the multiple measurements make it possible to estimate not only the target's position and its kinematics (speed, heading, etc), but also to estimate the target's extent in the measurement domain, i.e. to estimate the shape, the size and the orientation of the target. To estimate the target's extent requires a measurement model that relates the multiple measurements to the states that govern the extent.

Spatial distribution models in extended target tracking appeared in [6], [7]. Under this model each extended target measurement is a random sample from a probability distribution that is dependent on the extended target state. A number of different extended target models have been presented, where the targets are modeled as sticks, ellipses, rectangles, or general shapes, see e.g. [2], [9], [17], [20].

In the random matrix extended target model, originally proposed in [17], the extended target state is the combination of a kinematic state vector $\mathbf{x}_k$ and an extent matrix X_k. The vector $\mathbf{x}_k$ represents the target's position and kinematics, and the matrix X_k represents the target's size and shape, i.e. its spatial extent. The matrix X_k is modeled as being symmetric and positive definite, which implies that the target shape is approximated by an ellipse. The random matrix model was modified in [5] to allow for a more general class of kinematic vectors. Additional work on the measurement update and prediction update can be found in [14], [18], [23]. Estimation of multiple objects within the random matrix framework can be found in [11], [19], [21], [24]–[26].

In this paper we consider state estimation for extended targets whose extents cannot be approximated by a simple geometric shape such as an ellipse or a rectangle. Multiple ellipses are used to describe the shape and size of a single extended target. Using multiple simple shapes alleviates the limitations posed by the implied elliptic target shape[1], and also retains, on a subobject level, the simplicity of the random matrix model [5], [17].

The extended target is modeled as a collection of elliptical subobjects, see Fig. 1, and the positions and extents of the subobjects are Gaussian inverse Wishart distributed. The scope of the paper is limited by the assumptions that *a*) there is exactly one target present; *b*) there are no clutter measurements; and *c*) the number of subobjects is constant and known. To handle multiple targets and clutter, the presented work can be integrated into a multiple target framework, e.g. an extended target PHD/CPHD filter [8], [10], [11], [21], [22]. Estimating the number of subobjects is left for future work.

[1]As the number of ellipses grows, their combination can form nearly any given shape.

TABLE I
NOTATIONS

- $\mathbb{R}^n$ is the set of real column vectors of length n, $\mathbb{S}^n_{++}$ is the set of symmetric positive definite $n \times n$ matrices, $\mathbb{S}^n_{+}$ is the set of symmetric positive semi-definite $n \times n$ matrices, and $\mathbb{N}$ is the set of non-negative integers.
- $\mathbf{I}_d$ is a $d \times d$ identity matrix, $\mathbf{1}_{d \times e}$ is a $d \times e$ all-one matrix, and $\mathbf{0}_{d \times e}$ is a $d \times e$ all-zero matrix.
- $|\cdot|$ is absolute value, $\|\cdot\|_2$ is Euclidean norm, and $\|\cdot\|_F$ is Frobenius norm.
- $A \otimes B$ is Kronecker product for matrices A and B.
- $\mathcal{PS}(n;\ \gamma)$ denotes a Poisson probability mass function (pmf) over the integer $n \in \mathbb{N}$ with rate parameter $\gamma > 0$.
- $\mathcal{G}(\gamma\,;\,\alpha, \beta)$ denotes a Gamma probability density function (pdf) over the scalar $\gamma > 0$ with scalar shape parameter $\alpha > 0$ and scalar inverse scale parameter $\beta > 0$.
- $\mathcal{N}(\mathbf{x}\,;\,\mathbf{m}, P)$ denotes a multi-variate Gaussian pdf over the vector $\mathbf{x} \in \mathbb{R}^{n_x}$ with mean vector $\mathbf{m} \in \mathbb{R}^{n_x}$, and covariance matrix $P \in \mathbb{S}^{n_x}_{+}$.
- $\mathcal{IW}_d(X\,;\,v, V)$ denotes an inverse Wishart pdf over the matrix $X \in \mathbb{S}^d_{++}$ with scalar degrees of freedom $v > 2d$ and parameter matrix $V \in \mathbb{S}^d_{++}$, see, e.g. [16, Definition 3.4.1].
- $\mathcal{W}_d(X\,;\,w, W)$ denotes a Wishart pdf over the matrix $X \in \mathbb{S}^d_{++}$ with scalar degrees of freedom $w \geq d$ and parameter matrix $W \in \mathbb{S}^d_{++}$, see, e.g. [16, Definition 3.2.1].

The rest of the paper is outlined as follows. The next section presents the proposed extended target model, and gives a gamma Gaussian inverse Wishart implementation. In Section III some implementation issues are presented. A simulation study is presented in Section IV, and the paper is concluded in Section V.

II. PROPOSED MULTIPLE ELLIPSE MODEL

In this section we introduce the new extended target model. Some notation is given in Table I.

A. Extended target state

The extended target is made up of a combination of N_s d-dimensional subobjects, where N_s is constant and known. Each subobject i is described by a position $\mathbf{p}_k^{(i)} \in \mathbb{R}^d$, a measurement rate[2] $\gamma_k^{(i)} > 0$ and an extent state $X_k^{(i)} \in \mathbb{S}^d_{++}$, where sub-index k refers to discrete time step t_k. The number of measurements per time step from a subobject is modeled as Poisson distributed with measurement rate $\gamma_k^{(i)} > 0$ [6], [7]. The extent describes the size and the shape of the subobject; within the random matrix framework the shape is an ellipse.

Because extended targets in most cases can be assumed to be rigid bodies the subobjects have unified dynamics, by which we mean that all subobjects move forward with the same speed and the same heading, turn with the same turn-rate, etc. The unified dynamics vector is $\mathbf{c}_k = \begin{bmatrix}\mathbf{v}_k^{\mathrm{T}} & \omega_k\end{bmatrix}^{\mathrm{T}} \in \mathbb{R}^{n_c}$, where $\mathbf{v}_k \in \mathbb{R}^d$ is the Cartesian velocity vector and ω_k is the turn-rate. The turn-rate is defined w.r.t. the extended target's center of mass $\mathbf{p}_k^c$,

$$\mathbf{p}_k^c = \frac{1}{N_s}\sum_{i=1}^{N_s}\mathbf{p}_k^{(i)}. \tag{1}$$

[2]In this paper the term *measurement rate* denotes the number of measurements generated by the subobject.

Note that $\mathbf{c}_k$ can be extended to also include parameters for individual subobject dynamics. This would be useful for group tracking, where the individual targets in the group may shift their positions within the group.

Because the extended target is a rigid body, a detection from one of the subobjects will contain information not only about that subobject but also about all other subobjects. It is therefore important to model the subobject positions $\mathbf{p}_k^{(i)}$ and unified dynamics as a single state, such that the correlations between the positions and the kinematics can be estimated. In this work the positions and dynamics of all subobjects are jointly described by a kinematic state $\mathbf{x}_k \in \mathbb{R}^{n_x}$,

$$\mathbf{x}_k = \left[\left(\mathbf{p}_k^{(1)}\right)^{\mathrm{T}} \quad \ldots \quad \left(\mathbf{p}_k^{(N_s)}\right)^{\mathrm{T}} \quad \mathbf{c}_k^{\mathrm{T}}\right]^{\mathrm{T}}. \tag{2}$$

For brevity the measurement rates, kinematic state and extent states are abbreviated as follows

$$\xi_k = \left(\gamma_k^{(1)}, \ldots, \gamma_k^{(N_s)}, \mathbf{x}_k, X_k^{(1)}, \ldots, X_k^{(N_s)}\right) \tag{3}$$

where ξ_k is referred to as the extended target state. Let $\mathbf{Z}_k$ be a set of target generated measurements $\mathbf{Z}_k = \{\mathbf{z}_k^{(j)}\}_{j=1}^{n_{z,k}}$, where $n_{z,k}$ is the number of measurements, $\mathbf{z}_k^{(j)} \in \mathbb{R}^d$, $\forall j$, and let $\mathbf{Z}^k$ be a sequence of measurement sets from time t_0 to time t_k.

The distribution of the extended target state ξ_k, conditioned on the history of measurement sets, is represented by a distribution mixture

$$p\left(\xi_k \left| \mathbf{Z}^k\right.\right) = \sum_{\ell=1}^{J_{k|k}} w_{k|k}^{(\ell)} \mathcal{GGIW}\left(\xi_k\,;\,\zeta_{k|k}^{(\ell)}\right), \tag{4}$$

where $J_{k|k}$ is the number of mixture components, $\sum_\ell w_{k|k}^{(\ell)} = 1$ and $\mathcal{GGIW}(\,\cdot\,;\,\cdot\,)$ denotes the Gamma Gaussian inverse Wishart density,

$$\begin{aligned}\mathcal{GGIW}\left(\xi_k\,;\,\zeta_{k|k}\right) &= \mathcal{N}\left(\mathbf{x}_k\,;\,m_{k|k}, P_{k|k}\right) \\ &\times \prod_{i=1}^{N_s}\left(\mathcal{G}\left(\gamma_k^{(i)}\,;\,\alpha_{k|k}^{(i)}, \beta_{k|k}^{(i)}\right)\mathcal{IW}_d\left(X_k^{(i)}\,;\,v_{k|k}^{(i)}, V_{k|k}^{(i)}\right)\right)\end{aligned} \tag{5}$$

$\zeta_{k|k}$ is an abbreviation of all the parameters involved.

B. Prediction

To handle different types of motion M_k different motion models are used. With a posterior distribution of the form (4) the predicted distribution is

$$p\left(\xi_{k+1} \left| \mathbf{Z}^k\right.\right) = \sum_{m=1}^{M_k}\sum_{\ell=1}^{J_{k|k}} \pi_{m,m'(\ell)} w_{k|k}^{(\ell)} \mathcal{GGIW}\left(\xi_k\,;\,\zeta_{k+1|k}^{(m,\ell)}\right), \tag{6}$$

where $\pi_{m,m'(\ell)}$ is the probability of a transition to the current mode m from the previous mode $m'(\ell)$ that component ℓ was in.

1) Measurement rates: For the mth motion mode the parameters are predicted as

$$\alpha_{k+1|k}^{(m,\ell,i)} = \frac{\alpha_{k|k}^{(\ell,i)}}{\eta_k^{(m)}}, \qquad \beta_{k+1|k}^{(m,\ell,i)} = \frac{\beta_{k|k}^{(\ell,i)}}{\eta_k^{(m)}}, \tag{7}$$

which corresponds to keeping the expected value of $\gamma_k^{(i)}$ constant, while increasing the variance with a factor $\eta_k^{(m)}$ [12]. This prediction is a type of exponential forgetting with an effective window length of $w_e = \frac{\eta_k^{(m)}}{\eta_k^{(m)}-1}$, where $\frac{1}{\eta_k^{(m)}} < 1$ is the forgetting factor.

2) Kinematic state: For the mth motion mode the kinematic state transition density is modeled as

$$p(\mathbf{x}_{k+1}|\mathbf{x}_k) = \mathcal{N}\left(\mathbf{x}_{k+1}\,;\, f^{(m)}(\mathbf{x}_k), Q_{k+1}^{(m)}\right) \tag{8}$$

The motion model describes a coordinated turn for the extended object,

$$f^{(m)}(\mathbf{x}_k) = g^{(m)}(\omega_k)\mathbf{x}_k + \mathbf{w}_k^{(m)} \tag{9a}$$

$$g^{(m)}(\omega_k) = \begin{bmatrix} L(\omega_k) & \mathbf{1}_{N_s\times 1}\otimes U(\omega_k) & \mathbf{0}_{2N_s\times 1} \\ \mathbf{0}_{2\times 2N_s} & R(\omega_k) & \mathbf{0}_{2\times 1} \\ \mathbf{0}_{1\times 2N_s} & \mathbf{0}_{1\times 2} & e^{-\alpha^{(m)}T} \end{bmatrix} \tag{9b}$$

$$L(\omega_k) = \frac{\mathbf{1}_{N_s\times N_s}\otimes \mathbf{I}_d}{N_s} + \left(\mathbf{I}_{N_s} - \frac{\mathbf{1}_{N_s\times N_s}}{N_s}\right)\otimes R(\omega_k) \tag{9c}$$

$$R(\omega_k) = \begin{bmatrix} \cos(T\omega_k) & -\sin(T\omega_k) \\ \sin(T\omega_k) & \cos(T\omega_k) \end{bmatrix} \tag{9d}$$

$$U(\omega_k) = \begin{bmatrix} \frac{\sin(T\omega_k)}{\omega_k} & -\frac{1-\cos(T\omega_k)}{\omega_k} \\ \frac{1-\cos(T\omega_k)}{\omega_k} & \frac{\sin(T\omega_k)}{\omega_k} \end{bmatrix} \tag{9e}$$

where T is the sample time. The process noise $\mathbf{w}_k^{(m)}$ is zero mean Gaussian with covariance

$$Q_k^{(m)} = \begin{bmatrix} \Upsilon_1^{(m)} & \Upsilon_2^{(m)} & \mathbf{0}_{2N\times 1} \\ (\Upsilon_2^{(m)})^{\mathrm{T}} & \upsilon_{xy}^{(m)} T^2 \mathbf{I}_2 & \mathbf{0}_{2\times 1} \\ \mathbf{0}_{1\times 2N} & \mathbf{0}_{1\times 2} & \upsilon_w^{(m)} \end{bmatrix} \tag{10a}$$

$$\Upsilon_1^{(m)} = \mathbf{1}_{N\times N}\otimes \frac{\upsilon_{xy}^{(m)} T^4}{4}\mathbf{I}_2 + Q_d^{(m)} \tag{10b}$$

$$\Upsilon_2^{(m)} = \mathbf{1}_{N\times 1}\otimes \frac{\upsilon_{xy}^{(m)} T^3}{2}\mathbf{I}_2 \tag{10c}$$

Using the extended Kalman filter prediction formulas the predicted mean $m_{k+1|k}^{(m,\ell)}$ and covariance $P_{k+1|k}^{(m,\ell)}$ are

$$m_{k+1|k}^{(m,\ell)} = f^{(m)}(m_{k|k}^{(\ell)}), \tag{11a}$$

$$P_{k+1|k}^{(m,\ell)} = F_{k|k}^{(m,\ell)} P_{k|k}^{(\ell)} \left(F_{k|k}^{(m,\ell)}\right)^{\mathrm{T}} + Q_{k+1}^{(m)} \tag{11b}$$

where $F_{k|k}^{(m,\ell)} = \nabla_{\mathbf{x}} f^{(m)}(\mathbf{x})\big|_{\mathbf{x}=m_{k|k}^{(\ell)}}$ is the gradient of $f^{(m)}(\,\cdot\,)$ evaluated at the mean $m_{k|k}^{(\ell)}$.

3) Random matrices: For the mth motion mode we use the transition density

$$\begin{aligned} &p(X_{k+1}^{(i)}|\mathbf{x}_k, X_k^{(i)}) \\ &= \mathcal{W}_d\left(X_{k+1}^{(i)}\,;\, n_{k+1}^{(m)}, \left(n_{k+1}^{(m)}\right)^{-1} R(\omega_k) X_k^{(i)} R(\omega_k)^{\mathrm{T}}\right), \end{aligned} \tag{12}$$

where $n_{k+1}^{(m)} > d-1$ is a scalar design parameter and the matrix transformation $M_{\mathbf{x}_k}^{(m)} \triangleq$ is a rotation matrix. Details on how the parameters $v_{k+1|k}^{(m,\ell,i)}$ and $V_{k+1|k}^{(m,\ell,i)}$ are computed are given in [14].

C. Update

Let θ denote a possible measurement-to-subobject association event, and let $\boldsymbol{\Theta}$ denote the set of all possible association events. For measurement generation, we assume the following:

Assumption 1: The subobjects generate measurements independently of each other. For each subobject, the generated measurements are independent. Each measurement is generated by exactly one subobject. Measurement origin is unknown. □

Remark: These assumptions are analogous to standard assumptions in multiple target tracking, see e.g. [1]. □

Under an association event θ the measurement set $\mathbf{Z}_k$ can be partitioned into N_s (possibly empty) subsets that correspond to the association events θ,

$$\mathbf{Z}_k = \bigcup_{i=1}^{N_s} \mathbf{Z}_k^{(\theta,i)}, \qquad \mathbf{Z}_k^{(\theta,i)} = \left\{\mathbf{z}_k^{(\theta,i,j)}\right\}_{j=1}^{n_{z,k}^{(\theta,i)}}, \tag{13}$$

where the ith subset $\mathbf{Z}_k^{(\theta,i)}$ was generated by the ith subobject. Conditioned on θ the measurement likelihood is

$$p\left(\mathbf{Z}_k\,|\xi_k,\theta\right) = \prod_{i=1}^{N_s} p\left(\mathbf{Z}_k^{(\theta,i)}\,\middle|\,\gamma_k^{(i)}, \mathbf{x}_k, X_k^{(i)}\right). \tag{14}$$

If the ith subset is empty (i.e. $n_{z,k}^{(\theta,i)} = 0$) the subset likelihood is simply the likelihood of an empty set of measurements,

$$p\left(\mathbf{Z}_k^{(\theta,i)}\,\middle|\,\gamma_k^{(i)}, \mathbf{x}_k, X_k^{(i)}\right) = \mathcal{PS}\left(0;\ \gamma_k^{(i)}\right). \tag{15}$$

If $n_{z,k}^{(\theta,i)} > 0$ the subobject likelihood is

$$\begin{aligned} &p\left(\mathbf{Z}_k^{(\theta,i)}\,\middle|\,\gamma_k^{(i)}, \mathbf{x}_k, X_k^{(i)}\right) \\ &= n_{z,k}^{(\theta,i)}!\,\mathcal{PS}\left(n_{z,k}^{(i)};\ \gamma_k^{(i)}\right) \prod_{j=1}^{n_{z,k}^{(\theta,i)}} \mathcal{N}\left(\mathbf{z}_k^{(i,j)}\,;\, H_k^{(i)}\mathbf{x}_k, X_k^{(i)}\right). \end{aligned} \tag{16}$$

where the measurement models $H_k^{(i)}$ are

$$H_k^{(i)} = \begin{bmatrix} \mathbf{0}_{d\times(i-1)d} & \mathbf{I}_d & \mathbf{0}_{d\times(N_s-i)d} & \mathbf{0}_{d\times n_c} \end{bmatrix}, \tag{17}$$

for $i = 1, \ldots, N_s$.

Let the predicted mixture distribution be

$$p\left(\xi_k\,|\mathbf{Z}^{k-1}\right) = \sum_{\ell=1}^{J} w^{(\ell)} p^{(\ell)}\left(\xi_k\,|\mathbf{Z}^{k-1}\right). \tag{18}$$

By the total probability theorem the density $p\left(\xi_k|\mathbf{Z}^k\right)$ is

$$p\left(\xi_k|\mathbf{Z}^k\right) = \sum_{\theta\in\boldsymbol{\Theta}} p\left(\xi_k|\mathbf{Z}^k,\theta\right) P\left(\theta|\mathbf{Z}^k\right), \tag{19}$$

where $p\left(\xi_k|\mathbf{Z}^k,\theta\right)$ is the Bayes updated distribution for the association event θ, and $P\left(\theta|\mathbf{Z}^k\right)$ is the probability of the association event θ. Without any prior information the association events can be assumed to be equally likely, i.e. $P\left(\theta|\mathbf{Z}^{k-1}\right) = |\mathbf{\Theta}|^{-1}$. In this case we have

$$P\left(\theta|\mathbf{Z}^{k}\right) = \frac{\sum_{\ell=1}^{J} w^{(\ell)} p^{(\ell)}\left(\mathbf{Z}_k|\theta,\mathbf{Z}^{k-1}\right)}{\sum_{\theta'\in\mathbf{\Theta}}\sum_{\ell'=1}^{J} w^{(\ell')} p^{(\ell')}\left(\mathbf{Z}_k|\theta',\mathbf{Z}^{k-1}\right)}, \tag{20}$$

where we have again used the total probability theorem. For the association event θ the Bayes updated distribution is

$$p\left(\xi_k\left|\mathbf{Z}^{k},\theta\right.\right) = \frac{\sum_{\ell=1}^{J} w^{(\ell)} p^{(\ell)}\left(\mathbf{Z}_k\left|\theta,\mathbf{Z}^{k-1}\right.\right) p^{(\ell)}\left(\xi_k\left|\mathbf{Z}^{k},\theta\right.\right)}{\sum_{\ell=1}^{J} w^{(\ell)} p^{(\ell)}\left(\mathbf{Z}_k\left|\theta,\mathbf{Z}^{k-1}\right.\right)}. \tag{21}$$

Combining (18), (19), (20) and (21) gives the posterior distribution

$$p\left(\xi_k|\mathbf{Z}^{k}\right) = \sum_{\theta\in\mathbf{\Theta}}\sum_{\ell=1}^{J} w^{(\ell)}\left(\theta\right) p^{(\ell)}\left(\xi_k\left|\mathbf{Z}^{k},\theta\right.\right), \tag{22}$$

$$w^{(\ell)}\left(\theta\right) = \frac{w^{(\ell)} p^{(\ell)}\left(\mathbf{Z}_k|\theta,\mathbf{Z}^{k-1}\right)}{\sum_{\theta'\in\mathbf{\Theta}}\sum_{\ell'=1}^{J} w^{(\ell')} p^{(\ell')}\left(\mathbf{Z}_k|\theta',\mathbf{Z}^{k-1}\right)}, \tag{23}$$

where, following the assumption that the subobjects generate measurements independently, for the predicted pdf of $\mathbf{Z}_k$ we have

$$p^{(\ell)}\left(\mathbf{Z}_k|\theta,\mathbf{Z}^{k-1}\right) = \prod_{i=1}^{N_s} p^{(\ell)}\left(\mathbf{Z}_k^{(\theta,i)}\middle|\mathbf{Z}^{k-1}\right). \tag{24a}$$

$$p\left(\mathbf{Z}_k|\mathbf{Z}^{k-1}\right) = \frac{1}{|\mathbf{\Theta}|}\sum_{\theta\in\mathbf{\Theta}}\sum_{\ell=1}^{J} w^{(\ell)} p^{(\ell)}\left(\mathbf{Z}_k|\theta,\mathbf{Z}^{k-1}\right), \tag{24b}$$

The predicted pdf $p\left(\mathbf{Z}_k|\mathbf{Z}^{k-1}\right)$ is useful in a multiple target tracking scenario, e.g. if the presented extended target model is used in an implementation of an extended target PHD or CPHD filter [21], [22].

For an association event $\theta \in \mathbf{\Theta}$ the centroid measurement and scatter matrix are defined as follows,

$$\bar{\mathbf{z}}_k^{(\theta,i)} = \frac{1}{n_{z,k}^{(\theta,i)}}\sum_{j=1}^{n_{z,k}^{(\theta,i)}} \mathbf{z}_k^{(\theta,i,j)}, \tag{25a}$$

$$Z_k^{(\theta,i)} = \sum_{j=1}^{n_{z,k}^{(\theta,i)}}\left(\mathbf{z}_k^{(\theta,i,j)} - \bar{\mathbf{z}}_k^{(\theta,i)}\right)\left(\mathbf{z}_k^{(\theta,i,j)} - \bar{\mathbf{z}}_k^{(\theta,i)}\right)^{\mathrm{T}}. \tag{25b}$$

The same measurement model is used for all motion models. With a predicted distribution

$$p\left(\xi_k\left|\mathbf{Z}^{k-1}\right.\right) = \sum_{\ell=1}^{J_{k|k-1}} w_{k|k-1}^{(\ell)}\mathcal{GGIW}\left(\xi_k\,;\,\zeta_{k|k-1}^{(\ell)}\right) \tag{26}$$

the corrected distribution is

$$p\left(\xi_k\left|\mathbf{Z}^{k}\right.\right) = \sum_{\theta\in\mathbf{\Theta}}\sum_{\ell=1}^{J_{k|k-1}} w_{k|k}^{(\theta,\ell)}\mathcal{GGIW}\left(\xi_k\,;\,\zeta_{k|k}^{(\theta,\ell)}\right) \tag{27}$$

Next we give the measurement updated parameters and predicted likelihood for the measurement model described above. Due to page length restrictions the details of the proof are not given here but can be found in [15].

1) Measurement rates:

$$\alpha_{k|k}^{(\theta,\ell,i)} = \alpha_{k|k-1}^{(\ell,i)} + n_{z,k}^{(\theta,i)}, \qquad \beta_{k|k}^{(\theta,\ell,i)} = \beta_{k|k-1}^{(\ell,i)} + 1. \tag{28}$$

2) Kinematic state:

$$m_{k|k}^{(\theta,\ell)} = m_{k|k-1}^{(\ell)} + K_k^{(\theta,\ell)}\left(\bar{\mathbf{z}}_k^{(\theta)} - \mathbb{H}_k m_{k|k-1}^{(\ell)}\right), \tag{29a}$$

$$P_{k|k}^{(\theta,\ell)} = P_{k|k-1}^{(\ell)} + K_k^{(\theta,\ell)}\mathbb{H}_k P_{k|k-1}^{(\ell)}, \tag{29b}$$

$$\bar{\mathbf{z}}_k^{(\theta)} = \left[\left(\bar{\mathbf{z}}_k^{(\theta,1)}\right)^{\mathrm{T}} \quad \cdots \quad \left(\bar{\mathbf{z}}_k^{(\theta,N_s)}\right)^{\mathrm{T}}\right]^{\mathrm{T}}, \tag{29c}$$

$$\mathbb{H}_k = \left[\left(H_k^{(1)}\right)^{\mathrm{T}} \quad \cdots \quad \left(H_k^{(N_s)}\right)^{\mathrm{T}}\right]^{\mathrm{T}}, \tag{29d}$$

$$K_k^{(\theta,\ell)} = P_{k|k-1}^{(\ell)}\mathbb{H}_k^{\mathrm{T}}\left(S_k^{(\theta,\ell)}\right)^{-1}, \tag{29e}$$

$$S_k^{(\theta,\ell)} = \mathbb{H}_k P_{k|k-1}^{(\ell)}\mathbb{H}_k^{\mathrm{T}} + \hat{\mathbb{X}}_{k|k-1}^{(\theta,\ell)}, \tag{29f}$$

$$\hat{\mathbb{X}}_{k|k-1}^{(\theta,\ell)} = \mathrm{blkdiag}\left(\frac{\hat{X}_{k|k-1}^{(\ell,1)}}{n_{z,k}^{(\theta,1)}},\ldots,\frac{\hat{X}_{k|k-1}^{(\ell,N_s)}}{n_{z,k}^{(\theta,N_s)}}\right), \tag{29g}$$

$$\hat{X}_{k|k-1}^{(\ell,i)} = \frac{V_{k|k-1}^{(\ell,i)}}{v_{k|k-1}^{(\ell,i)} - 2d - 2}. \tag{29h}$$

3) Random matrices:

$$v_{k|k}^{(\theta,\ell,i)} = v_{k|k-1}^{(\ell,i)} + n_{z,k}^{(\theta,i)}, \tag{30a}$$

$$V_{k|k}^{(\theta,\ell,i)} = V_{k|k-1}^{(\ell,i)} + Z_k^{(\theta,i)} + N_{k|k-1}^{(\theta,\ell,i)}, \tag{30b}$$

$$N_{k|k-1}^{(\theta,\ell,i)} = \left(\hat{X}_{k|k-1}^{(\ell,i)}\right)^{\frac{1}{2}}\left(S_k^{(\theta,\ell,i)}\right)^{-\frac{1}{2}}\varepsilon_{k|k-1}^{(\theta,\ell,i)} \times\left(\varepsilon_{k|k-1}^{(\theta,\ell,i)}\right)^{\mathrm{T}}\left(S_k^{(\theta,\ell,i)}\right)^{-\frac{\mathrm{T}}{2}}\left(\hat{X}_{k|k-1}^{(\ell,i)}\right)^{\frac{\mathrm{T}}{2}}, \tag{30c}$$

$$\varepsilon_{k|k-1}^{(\theta,\ell,i)} = \bar{\mathbf{z}}_k^{(\theta,i)} - H_k^{(i)} m_{k|k-1}^{(\ell)}, \tag{30d}$$

$$S_k^{(\theta,\ell,i)} = H_k^{(i)} P_{k|k-1}^{(\ell)}\left(H_k^{(i)}\right)^{\mathrm{T}} + \frac{\hat{X}_{k|k-1}^{(\ell,i)}}{n_{z,k}^{(\theta,i)}}, \tag{30e}$$

Matrix square-roots are computed using, e.g., Cholesky factorization.

4) Weights:

$$w_{k|k}^{(\theta,\ell)} = \frac{w_{k|k-1}^{(\ell)}\prod_{i=1}^{N_s}\mathcal{L}_k^{(\theta,\ell,i)}}{\sum_{\theta'\in\bar{\mathbf{\Theta}}}\sum_{\ell'=1}^{J_{k|k-1}} w_{k|k-1}^{(\ell')}\prod_{i'=1}^{N_s}\mathcal{L}_k^{(\theta',\ell',i')}}, \tag{31a}$$

$$\mathcal{L}_k^{(\theta,\ell,i)} = \frac{\Gamma\left(\alpha_{k|k}^{(\theta,\ell,i)}\right)}{\Gamma\left(\alpha_{k|k-1}^{(\ell,i)}\right)}\frac{\left(\beta_{k|k-1}^{(\ell,i)}\right)^{\alpha_{k|k-1}^{(\ell,i)}}}{\left(\beta_{k|k}^{(\theta,\ell,i)}\right)^{\alpha_{k|k}^{(\theta,\ell,i)}}} \times\frac{\left(n_{z,k}^{(\theta,i)}\pi^{n_{z,k}^{(\theta,i)}}\right)^{-\frac{d}{2}} 2^{-\frac{n_{z,k}^{(\theta,i)}(d-1)}{2}}}{\left|\left(\hat{X}_{k|k-1}^{(\ell,i)}\right)^{-\frac{1}{2}} S_k^{(\theta,\ell,i)}\left(\hat{X}_{k|k-1}^{(\ell,i)}\right)^{-\frac{\mathrm{T}}{2}}\right|^{\frac{1}{2}}} \times\frac{\Gamma_d\left(\frac{v_{k|k}^{(\theta,\ell,i)}-d-1}{2}\right)}{\Gamma_d\left(\frac{v_{k|k-1}^{(\ell,i)}-d-1}{2}\right)}\frac{\left|V_{k|k-1}^{(\ell,i)}\right|^{\frac{v_{k|k-1}^{(\ell,i)}-d-1}{2}}}{\left|V_{k|k}^{(\theta,\ell,i)}\right|^{\frac{v_{k|k}^{(\theta,\ell,i)}-d-1}{2}}}. \tag{31b}$$

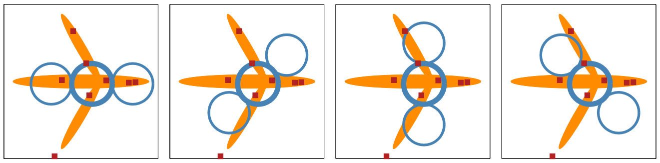

Fig. 2. Initialization example. True underlying extended target (orange area), measurements (red squares), and initialized estimates (blue ellipses).

TABLE II
MULTIPLE ELLIPSE PARAMETER INITIALIZATION

Input: Set of measurements $\mathbf{Z} = \{\mathbf{z}_i\}_{i=1}^{n}$. Desired number of initial hypotheses N_p. Initial kinematics $\mathbf{c}_0$ and initial covariance P_0. Initial mean e and variance v for measurement rates.
$\mathbf{z}_c = \frac{1}{n}\sum_{i=1}^{n}\mathbf{z}_i$, $r_z = \frac{1}{2}\max_i \|\mathbf{z}_i - \mathbf{z}_c\|_2$, $\Sigma_0 = \left(\frac{r_z}{4}\right)^2 \mathbf{I}_d$, $\ell = 0$.
for $p = 1, \ldots, N_p$ **do**
  for $m = 1, \ldots, M_k$ **do**
    Set $\ell = \ell + 1$
    γ: $\alpha_0^{(\ell,i)} = \frac{e^2}{v}$, $\beta_0^{(\ell,i)} = \frac{e}{v}$.
    $\mathbf{x}$: $P_0^{(\ell)} = P_0$, $\mathbf{c}_0^{(\ell)} = \mathbf{c}_0$,

$$\mathbf{p}_0^{(\ell,i)} = \mathbf{z}_c + r_z \begin{bmatrix} \cos\left(\frac{2\pi(i-1)}{N_s} + \frac{2\pi(p-1)}{N_s N_p}\right) \\ \sin\left(\frac{2\pi(i-1)}{N_s} + \frac{2\pi(p-1)}{N_s N_p}\right) \end{bmatrix}.$$

    X: $v_0^{(\ell,i)} = 2d+5$, $V_0^{(\ell,i)} = \Sigma_0\left(v_0^{(\ell,i)} - 2d - 2\right)$.
  end for
end for
Output: $p(\xi_0) = \sum_{\ell=1}^{J_0} w_0^{(\ell)} \mathcal{GGIW}\left(\xi_0\,;\,\zeta_0^{(\ell)}\right)$ where $w_0^{(\ell)} = \frac{1}{J_0}$.

5) Predicted observation pdfs:

$$p^{(\ell)}\left(\mathbf{Z}_k|\theta, \mathbf{Z}^{k-1}\right) = \prod_{i=1}^{N_s} \mathcal{L}_k^{(\theta,\ell,i)} \tag{32a}$$

$$p\left(\mathbf{Z}_k|\mathbf{Z}^{k-1}\right) = \frac{1}{|\bar{\mathbf{\Theta}}|}\sum_{\theta\in\bar{\mathbf{\Theta}}}\sum_{\ell=1}^{J_{k|k-1}} w_{k|k-1}^{(\ell)} \prod_{i=1}^{N_s}\mathcal{L}_k^{(\theta,\ell,i)}. \tag{32b}$$

III. Implementation Issues

A. Estimate initialization

When a new target appears the parameters $\zeta^{(\ell)}$ of the estimate must be initialized. Table II gives a simple algorithm where this is performed using the first set of measurements. The algorithm initializes N_p hypotheses in each motion mode. A simple initialization example is given in Figure 2. In this example there is a single motion mode, and $N_p = 4$ hypotheses are generated using only 8 measurements.

B. Generation of association events

For $n_{z,k}$ measurements and N_s subobjects there are $(N_s)^{n_{z,k}}$ possible measurement-to-subobject association events. Due to the quickly increasing size of the full set of association events approximations are necessary to achieve tractable computational complexity.

In this paper a subset $\bar{\mathbf{\Theta}} \subseteq \mathbf{\Theta}$ of association events is computed using a method that is based on the Expectation Maximization algorithm [4] for Gaussian Mixtures (EM-GM), see e.g. [3, Chapter 9]. First EM-GM is used to partition the current set of measurements into N_c clusters, where $N_c \in [1, 2, \ldots, N_s]$. Because EM-GM may have multiple stationary points, for each N_c the algorithm is given several different initializations. Note that care is taken to ensure that the set of partitions returned by EM-GM only contains unique partitions.

The next step is to use the clusters to obtain measurement-to-subobject associations. Given a partition of the measurement set with N_c clusters, and an estimate with N_s subobjects, there are $N_s!/(N_s - N_c)!$ possible cluster-to-subobject associations. A cluster-to-subobject association defines a measurement-to-subobject association event θ because each measurement is associated to a cluster, which in turn is associated to a subobject. Let $C(N_c)$ denote the number of unique partitions with N_c clusters obtained using EM-GM. Then the number of measurement-to-subobject association events that has to be considered is

$$\left|\bar{\mathbf{\Theta}}\right| = \sum_{N_c=1}^{N_s} C(N_c)\frac{N_s!}{(N_s - N_c)!}. \tag{33}$$

Empirically we have found that this number typically is several orders of magnitude smaller than $(N_s)^{n_{z,k}}$.

C. Mixture reduction

With $J_{k|k}$ components, M_k motion models and $|\bar{\mathbf{\Theta}}|$ association events there are $J_{k+1|k+1} = |\bar{\mathbf{\Theta}}| M_k J_{k|k}$ components after one iteration of prediction and correction. Mixture reduction is used in each iteration after the correction step to keep the number of components at a tractable level. Hypotheses with weights lower than a threshold τ are pruned and the weights are re-normalized. Merging is then performed on the mixture, where we have used a combination of the gamma mixture merging from [12] and the Gaussian inverse Wishart merging from [13]. Note that merging is only performed within the same motion modes, and not across the motion modes.

IV. Simulation Results

A. Target extraction and performance evaluation

To extract a target estimate from a mixture (4), additional merging is first performed, this time across the motion modes. Expected values of the measurement rates, positions and extent matrices are then computed w.r.t. the component with the highest weight $w_{k|k}^{(\ell)}$. Both the predicted estimate $\hat{\xi}_{k|k-1}$ and the filtered estimate $\hat{\xi}_{k|k}$ are compared to the true target state ξ_k. The following error metrics are used for the measurement rates, subobject positions, and random matrices,

$$d_{k|k}^{\gamma} = \sum_{i=1}^{N_s}\left|\gamma_k^{(i)} - \hat{\gamma}_{k|k}^{(\pi(i))}\right|, \ \hat{\gamma}_{k|k}^{(i)} = \mathrm{E}\left[\gamma_k^{(i)}\middle|\mathbf{Z}^k\right] \tag{34a}$$

$$d_{k|k}^{\mathbf{p}} = \sum_{i=1}^{N_s}\left\|\mathbf{p}_k^{(i)} - \hat{\mathbf{p}}_{k|k}^{(\pi(i))}\right\|_2, \ \hat{\mathbf{p}}_{k|k}^{(i)} = \mathrm{E}\left[\mathbf{p}_k^{(i)}\middle|\mathbf{Z}^k\right] \tag{34b}$$

$$d_{k|k}^{X} = \sum_{i=1}^{N_s}\left\|X_k^{(i)} - \hat{X}_{k|k}^{(\pi(i))}\right\|_F, \hat{X}_{k|k}^{(i)} = \mathrm{E}\left[X_k^{(i)}\middle|\mathbf{Z}^k\right] \tag{34c}$$

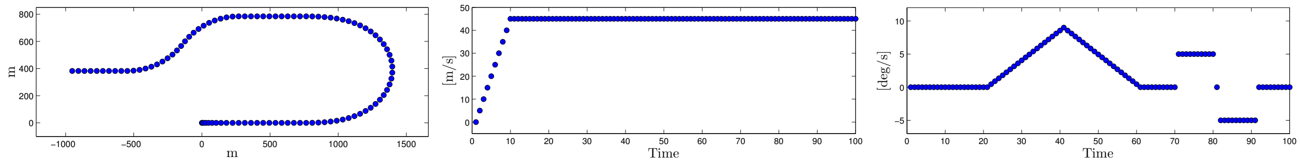

Fig. 3. True target trajectory, initial position is origin. Left: x, y-position. Middle: velocity. Right: turn rate.

A subobject-to-subobject association $\pi(i)$ is obtained by minimizing $d^{\mathbf{p}}_{k|k}$. Because $\gamma_k^{(i)}$, $\mathbf{p}_k^{(i)}$ and $X_k^{(i)}$ all have different units we refrain from computing an overall metric for the extended target state ξ_k.

B. True tracks and setup

The target trajectory that was simulated is shown in Fig. 3; true position (left), speed (middle) and turn rate (right).

Two different $d = 2$ dimensional extended target shapes were simulated. They consist of three and two subobjects, respectively. The shape of the targets are consistent with the examples given in Fig. 1, i.e. the shape resembles that of an airplane and of the letter V, respectively. For the plane-like target, for the subobject that corresponds to the fuselage the measurement rate was $2\gamma_0$, and the extent matrix was $X = \text{diag}\left([10^2\ ,\ 2^2]\right)$. For the subobjects that correspond to the wings the measurement rates were γ_0, and the extent matrices were $X = \text{diag}\left([5^2\ ,\ 1^2]\right)$. For the V-shaped target, the subobjects both had measurement rates γ_0 and extent matrices $X = \text{diag}\left([20^2\ ,\ 1^2]\right)$. The scenarios were simulated for different values of γ_0: 2, 5 and 20.

Two motion models were implemented, one with small process noise corresponding to non-maneuver, and one with larger process noise corresponding to maneuver. The transition probabilities were set to 95% probability to stay in the same mode, and 5% probability for mode switch.

The filter parameters that were used in the implementation are listed in Table III.

TABLE III
PARAMETERS FOR PROPOSED METHOD

Parameter		Value
Sample time	T	1
Number of initial hypotheses	N_p	$2(N_s-1)$
Initial kinematics	$\mathbf{c}_0$	$\mathbf{0}_{3\times 1}$
Initial covariance	P_0	$10^2\mathbf{I}_{n_x}$
Measurement rate initial mean	e	15
Measurement rate initial variance	v	10
Measurement rate prediction factor	$\eta_k^{(m)}$	1.05, $\forall m$
Exponential decay	$\alpha^{(m)}$	0 and 4
Acceleration noise	$v_{xy}^{(m)}$	2, $\forall m$
Prediction degrees of freedom	$n_{k+1}^{(m)}$	100, $\forall m$
Pruning threshold	τ	0.01

The proposed model, called MRMUK, is compared to a random matrix model that models each subobject individually and independently, i.e. individual kinematics instead of unified kinematics and the correclation between the subobjects' positions is not estimated. This model is denoted M2. Estimation of multiple independent elliptic objects can be found in [11], [19], [21], [24]–[26].

C. Results

The plane-shaped and the V-shaped targets were simulated for $\gamma_0 = 2$, $\gamma_0 = 5$, and $\gamma_0 = 20$. For each value of the measurement rate γ_0 the scenarios were simulated 10^3 times. For the plane-shaped target (three subobjects) the filter errors $d_{k|k}$ and prediction errors $d_{k|k-1}$ are shown in Fig. 4, for the V-shaped target (two subobjects) the results are shown in Fig. 5. Example filter and prediction outputs for the plane-shaped target for $\gamma_0 = 5$ are shown in Fig. 6. From the results the following observations can be made:

- Both the prediction errors and the filter errors are smaller for MRMUK than M2 for all γ_0.
- The biggest difference is for the subobject position errors, especially during maneuvers. Note that, even if the estimated random matrices have the correct size and orientation, the subobject positions are more important for the overall extended target extent estimate. The larger the subobject position errors are, the more distorted the overall shape becomes, which can be seen in Fig. 6.

The lower errors for MRMUK, especially the lower position errors, are a direct effect of *a*) using a single state vector for the subobject positions and the kinematics including a full covariance matrix; and *b*) having unified kinematics for the subobject positions.

D. Computational complexity

The code used in this work was implemented in MATLAB and run on a 2.83GHz Intel Core2 Quad CPU with 3.48GB of RAM running Windows. Note that the code has not been optimized for speed.

In each time step approximately 15 to 25 different partitions of the set of measurements were computed. The average number of measurement-to-subobject association events are

TABLE IV
NUMBER OF ASSOCIATION EVENTS, MEAN ± STANDARD DEVIATION

γ_0	$\lvert\bar{\Theta}\rvert$	$(N_s)^{\mathrm{E}[n_{z,k}]}$
2	114 ± 29	6.6×10^3
5	128 ± 24	3.5×10^9
20	130 ± 23	1.5×10^{38}

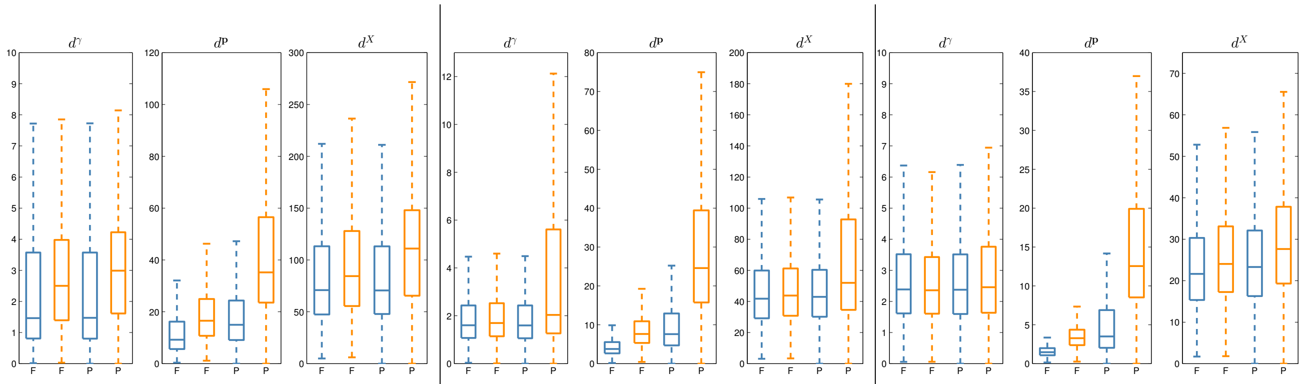

(a) $\gamma_0 = 2$ (b) $\gamma_0 = 5$ (c) $\gamma_0 = 20$

Fig. 4. Estimation errors for plane-shaped target. MRMUK in blue, model M2 in orange. x-labels F and P denote filter errors $d_{k|k}$ and prediction errors $d_{k|k-1}$. On each box, central mark is median, edges of box are 25th and 75th percentiles, whiskers extend to most extreme datapoints the algorithm considers to be not outliers.

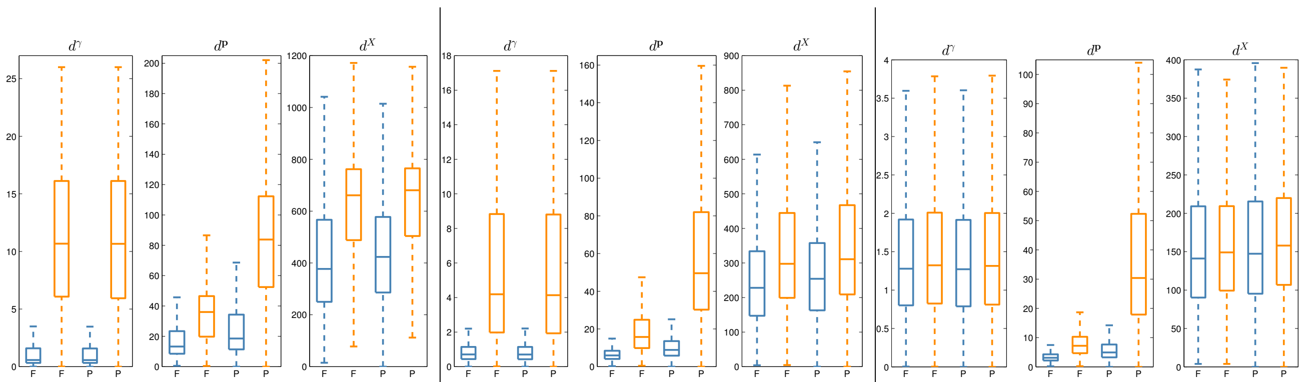

(a) $\gamma_0 = 2$ (b) $\gamma_0 = 5$ (c) $\gamma_0 = 20$

Fig. 5. Estimation errors for V-shaped target. MRMUK in blue, model M2 in orange. x-labels F and P denote filter errors $d_{k|k}$ and prediction errors $d_{k|k-1}$. On each box, central mark is median, edges of box are 25th and 75th percentiles, whiskers extend to most extreme datapoints the algorithm considers to be not outliers.

given in Table IV. A comparison to the number of association events if there are $\mathrm{E}[n_{z,k}]$ measurements shows that the set of association events is reduced by several orders of magnitude. It is noteworthy that for $\gamma_0 = 20$ the reduction in number of association events is by far greatest, yet the estimation errors are smaller for $\gamma_0 = 20$ than for $\gamma_0 = 2$ and $\gamma_0 = 5$.

The number of mixture components increase in each time step. However, in the mixture reduction step many components can be pruned, and the remaining components can be merged such that typically only 2 to 6 components remain.

The average cycle times are given in Table V. We see that the times for prediction and reduction are independent of γ_0. The time to compute clusters for data association increases when γ_0 increases, because with more measurements it takes more time to cluster them. The correction time decreases when γ_0 increases, because with more measurements the scenario is less ambiguous and the probability mixture typically has fewer components. Note that these two increases/decreases in time offset each other such that the average total cycle time is about 1.7 seconds for all values of γ_0 that were tested.

TABLE V

CYCLE TIMES [SECONDS], MEAN $\pm$ STANDARD DEVIATION

γ_0	Prediction	Clusters	Correction	Reduction	Total
2	0.4 ± 0.2	0.7 ± 0.1	0.6 ± 0.4	0.02 ± 0.02	1.7 ± 0.6
5	0.3 ± 0.1	0.9 ± 0.1	0.5 ± 0.3	0.01 ± 0.02	1.8 ± 0.4
20	0.2 ± 0.1	1.2 ± 0.1	0.3 ± 0.2	0.01 ± 0.02	1.7 ± 0.3

V. Conclusions and Future Work

The paper has presented an extended target model in which the target extent is modeled using a collection of elliptical sub-objects. The simulation results show that MRMUK outperforms work that does not model the unified kinematics and position correlations.

MRMUK can be reduced to the cases where either the measurement rates $\gamma_k^{(i)}$, the extent matrices $X_k^{(i)}$, or both, are known. The simulation study considered extended targets, however, the model is applicable also to group targets. In case the targets in the group are moving relative to each other, in addition to the unified group movement, individual kinematics can be estimated along with the unified kinematics.

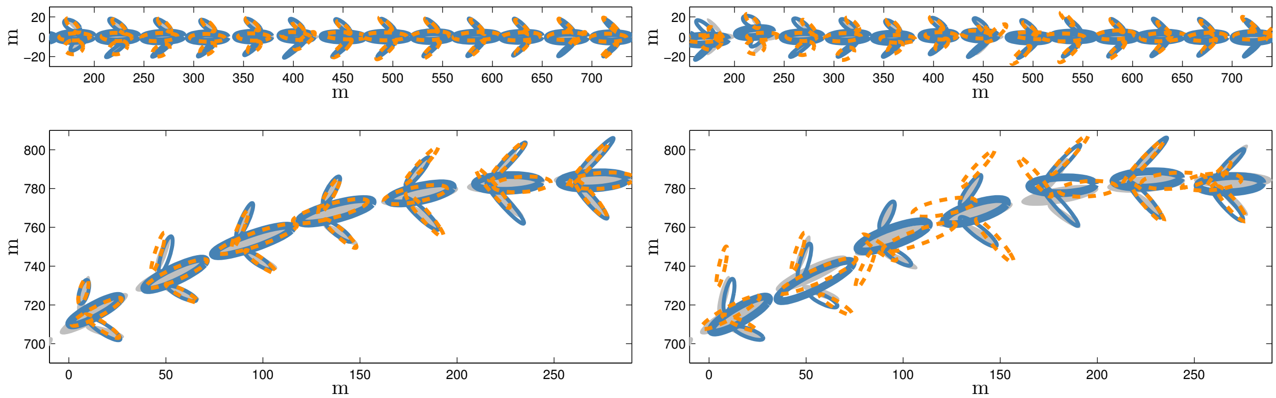

Fig. 6. Example results for $\gamma_0 = 5$ for the trajectory in Fig. 3. Left: filtered estimates. Right: predicted estimates. Ground truth (gray area), compared to model M2 (dashed orange line) and proposed method (solid blue line).

Acknowledgment

This research was supported by the Naval Postgraduate School, via ONR N00244-14-1-0033, and by ONR directly via N00014-13-1-0231; Y. Bar-Shalom is also supported by ARO W991NF-10-1-0369.

References

[1] Y. Bar-Shalom, P. K. Willett, and X. Tian, *Tracking and Data Fusion: A Handbook of Algorithms*. YBS Publishing, 2011.

[2] M. Baum and U. Hanebeck, "Extended object tracking with random hypersurface models," *IEEE Transactions on Aerospace and Electronic Systems*, vol. 50, no. 1, pp. 149–159, Jan. 2013.

[3] C. M. Bishop, *Pattern recognition and machine learning*. New York, USA: Springer, 2006.

[4] A. P. Dempster, N. M. Laird, and D. B. Rubin, "Maximum likelihood from incomplete data via the EM algorithm," *Journal of the Royal Statistical Society, Series B (Methodological)*, vol. 39, no. 1, pp. 1–38, 1977.

[5] M. Feldmann, D. Fränken, and J. W. Koch, "Tracking of extended objects and group targets using random matrices," *IEEE Transactions on Signal Processing*, vol. 59, no. 4, pp. 1409–1420, Apr. 2011.

[6] K. Gilholm, S. Godsill, S. Maskell, and D. Salmond, "Poisson models for extended target and group tracking," in *Proceedings of Signal and Data Processing of Small Targets*, vol. 5913. San Diego, CA, USA: SPIE, Aug. 2005, pp. 230–241.

[7] K. Gilholm and D. Salmond, "Spatial distribution model for tracking extended objects," *IEE Proceedings of Radar, Sonar and Navigation*, vol. 152, no. 5, pp. 364–371, Oct. 2005.

[8] K. Granström, C. Lundquist, and U. Orguner, "A Gaussian mixture PHD filter for extended target tracking," in *Proceedings of the International Conference on Information Fusion*, Edinburgh, UK, Jul. 2010.

[9] ——, "Tracking Rectangular and Elliptical Extended Targets Using Laser Measurements," in *Proceedings of the International Conference on Information Fusion*, Chicago, IL, USA, Jul. 2011, pp. 592–599.

[10] ——, "Extended Target Tracking using a Gaussian Mixture PHD filter," *IEEE Transactions on Aerospace and Electronic Systems*, vol. 48, no. 4, pp. 3268–3286, Oct. 2012.

[11] K. Granström and U. Orguner, "A PHD filter for tracking multiple extended targets using random matrices," *IEEE Transactions on Signal Processing*, vol. 60, no. 11, pp. 5657–5671, Nov. 2012.

[12] ——, "Estimation and Maintenance of Measurement Rates for Multiple Extended Target Tracking," in *Proceedings of the International Conference on Information Fusion*, Singapore, Jul. 2012, pp. 2170–2176.

[13] ——, "On the Reduction of Gaussian inverse Wishart mixtures," in *Proceedings of the International Conference on Information Fusion*, Singapore, Jul. 2012, pp. 2162–2169.

[14] ——, "A New Prediction Update for Extended Target Tracking with Random Matrices," *IEEE Transactions on Aerospace and Electronic Systems*, vol. 50, no. 2, Apr. 2014.

[15] K. Granström, "An extended target tracking model with multiple random matrices and unified kinematics," *CoRR*, vol. abs/1406.2135, 2014. [Online]. Available: http://arxiv.org/abs/1406.2135

[16] A. K. Gupta and D. K. Nagar, *Matrix variate distributions*, ser. Chapman & Hall/CRC monographs and surveys in pure and applied mathematics. Chapman & Hall, 2000.

[17] W. Koch, "Bayesian approach to extended object and cluster tracking using random matrices," *IEEE Transactions on Aerospace and Electronic Systems*, vol. 44, no. 3, pp. 1042–1059, Jul. 2008.

[18] J. Lan and X. Rong-Li, "Tracking of extended object or target group using random matrix – part I: New model and approach," in *Proceedings of the International Conference on Information Fusion*, Singapore, Jul. 2012, pp. 2177–2184.

[19] ——, "Tracking maneuvering non-ellipsoidal extended object or target group using random matrix," *IEEE Transactions on Signal Processing*, 2014.

[20] C. Lundquist, K. Granström, and U. Orguner, "Estimating the Shape of Targets with a PHD Filter," in *Proceedings of the International Conference on Information Fusion*, Chicago, IL, USA, Jul. 2011, pp. 49–56.

[21] ——, "An extended target CPHD filter and a gamma Gaussian inverse Wishart implementation," *IEEE Journal of Selected Topics in Signal Processing, Special Issue on Multi-target Tracking*, vol. 7, no. 3, pp. 472–483, Jun. 2013.

[22] R. Mahler, "PHD filters for nonstandard targets, I: Extended targets," in *Proceedings of the International Conference on Information Fusion*, Seattle, WA, USA, Jul. 2009, pp. 915–921.

[23] U. Orguner, "A variational measurement update for extended target tracking with random matrices," *IEEE Transactions on Signal Processing*, vol. 60, no. 7, pp. 3827–3834, Jul. 2012.

[24] M. Wieneke and S. Davey, "Histogram pmht with target extent estimates based on random matrices," in *Proceedings of the International Conference on Information Fusion*, Chicago, IL, USA, Jul. 2011, pp. 1–8.

[25] M. Wieneke and W. Koch, "A PMHT approach for extended objects and object groups," *IEEE Transactions on Aerospace and Electronic Systems*, vol. 48, no. 3, pp. 2349–2370, 2012.

[26] W. Wieneke and J. W. Koch, "Probabilistic tracking of multiple extended targets using random matrices," in *Proceedings of SPIE Signal and Data Processing of Small Targets*, Orlando, FL, USA, Apr. 2010.